Philosophical Magazine

Interrelation of depletion and segregation in decomposition of nanoparticles

A.M. Gusak [a] , A.O. Kovalchuk [a] & B.B. Straumal [b c]

[a] Department of Physics, Cherkasy National University, 81,
Shevchenko blvd, Cherkasy, 18027, Ukraine

[b] Laboratory of Interfaces in Metals, Institute of Solid State
Physics, Russian Academy of Sciences, Chernogolovka, Moscow,
142432, Russia

[c] Institute of Nanotechnology, Karlsruhe Institute of Technology
(KIT), Hermann-von-Helmholtz-Platz 1, Eggenstein-Leopoldshafen,
76344, Germany
Version of record first published: 02 Jan 2013.

PLEASE SCROLL DOWN FOR ARTICLE

Taylor & Francis
Taylor & Francis Group

Interrelation of depletion and segregation in decomposition of nanoparticles

A.M. Gusak[a]*, A.O. Kovalchuk[a] and B.B. Straumal[b,c]

[a]*Department of Physics, Cherkasy National University, 81, Shevchenko blvd, Cherkasy 18027, Ukraine;* [b]*Laboratory of Interfaces in Metals, Institute of Solid State Physics, Russian Academy of Sciences, Chernogolovka, Moscow 142432, Russia;* [c]*Institute of Nanotechnology, Karlsruhe Institute of Technology (KIT), Hermann-von-Helmholtz-Platz 1, Eggenstein-Leopoldshafen 76344, Germany*

An analytical description of the interrelation of depletion, segregation and decomposition of a binary alloy in a nanosystem is presented. Size-induced shift of the decomposition cupola appears to be a sum of two terms. The first (related to depletion caused by new phase formation) is inversely proportional to the size R to the power of $\frac{3}{4}$. The second (related to segregation at external surface) represents the traditional $1/R$ dependence. Size-induced 'splitting' of the decomposition cupola is also predicted and analytically described.

Keywords: decomposition; nucleation; depletion; segregation; thermodynamics; nanostructure; size effect

1. Introduction

Recent developments in nanoscaled reactions – change of the observed phase spectrum in point contact reactions in metal-silicon nanosystems [1–3], in exothermic reactions of Ni–Al and Ni–Zr nanosystems [4,5], change of solubility in binary alloys after grain refinement to nanosize [6–12] – motivate revisiting the old problem of the size effect in phase transformations of binary nanosystems. This size effect is usually ascribed to the capillary effect (Gibbs–Thomson law) [13]. The chemical potential of a system with a curved interface shifts proportionally to the curvature (or inversely proportional to the radius, if the interface is purely spherical or purely cylindrical). Well-known examples are the size ($1/R$) effect for melting temperature and for the equilibrium concentration in the vicinity of a nanoparticle interface.

On the other hand, interface curvature is not the only peculiarity of nanoparticles. Another peculiarity is also very important for binary and multicomponent particles – it is a depletion effect leading to the shift of the solubility limit, with respect to the bulk phase diagram [14–16]. Moreover, the solute concentration in the parent phase, corresponding to the solubility limit, now significantly differs from the concentration in this same phase in the equilibrium two-phase state after phase separation within nanoparticle – 'thermodynamic hysteresis' (in the bulk case, these two concentrations coincide) [17].

---

*Corresponding author. Email: gusak@cdu.edu.ua

One more peculiarity is an influence of segregation on the bulk properties. This effect is also related to finite volume and significant fraction of surface atoms among all atoms of the nanoparticle. A well-known example is the dissolution of cementite after severe plastic deformation of steel due to nanograined structure formation, and a corresponding abrupt increase in the grain-boundary network able to accommodate the segregated carbon atoms without compound formation [7–9,18,19].

Unlike the capillary effect, the depletion and segregation effects in nanoparticles, up to now, have had only numerical description. For example, it was not clear if the shift of solubilities and of phase equilibria in nanoparticles obeys some power law or another kind of size dependence.

In this work, for the first time, we present an analytical description of the depletion that caused size effect on the phase diagrams of binary nanoalloys and its synergy with surface segregation. We discover the combination of two power laws – $R^{-3/4}$ and R^{-1} – for both shifts of the solubility limit and of equilibrium states under phase separation in nanoparticles.

As we just mentioned, the transformation-induced depletion of the nanosystem becomes important for binary and multicomponent systems, in which phase transformation is related to the concentration change. The reason for the depletion effect in phase transformation is rather transparent: to form a critical nucleus of phase beta, enriched in the B-component, the system should deplete the surrounding parent phase. If the volume of parent phase is limited (typically, nanosized), the system may just not have a sufficient number of B-atoms, needed for the viable nucleus of new, beta-phase. In terms of the dependence of the Gibbs free energy change on the nucleus/embryo size, it means that this dependence will be (in this case) monotonically increasing, without barrier and local or global second minimum (the first one corresponds to zero size of embryo) – curve 1 in Figure 1 (for details see [14–17]).

It means that at the concentration and temperature inside the decomposition cupola (miscibility gap) of the bulk samples, the nanosized systems may appear to be stable.
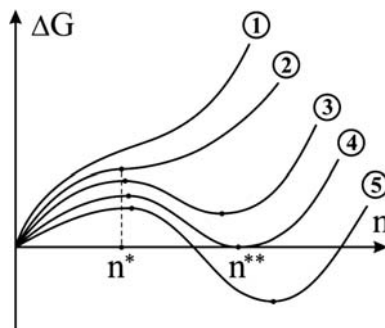
Figure 1. Qualitative dependence of the excess Gibbs free energy ΔG on the number of atoms n in the new phase nucleus at different total numbers of atoms in the particle ($N_1 < N_2 < N_3 < N_4 < N_5$): (1) – decomposition is impossible; (2) – marginal case, after which (with increasing particle size) decomposition becomes possible; (3) – decomposition is possible but unfavourable; 4 – marginal case, after which (with increasing particle size) decomposition becomes favourable; (5) – decomposition is possible and favourable (details can be found in [14–17, 20 chapter 13, 21]).

Figure 2. (a) Qualitative concentration dependence of the Gibbs free energy per atom of the parent phase α and of line compound phase i with $C_i = 1/2$. The composition C^{bin} of the bulk parent phase in the equilibrium with intermediate phase is determined by the common tangent. The driving force Δg of the bulk transformation is determined by the supersaturation magnitude. (b) Left half of corresponding phase diagram constructed according to common tangent rule.

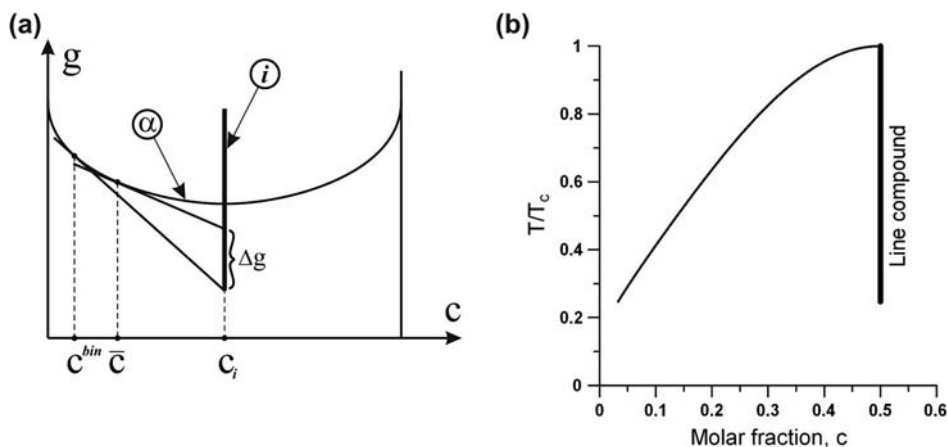So, one can expect the shift of solubility limits – actually, increasing solubility with decreasing particle size at any fixed temperature. On the other hand, after reaching and crossing the solubility limit and, hence, successful nucleation of new phase in the nanoparticle, the parent phase is significantly depleted (contrary to macroscopic systems, see below). So, it should be pointed out that after the decomposition in a particle has actually taken place, actual concentration in it becomes different from the concentration in the parent phase at which decomposition becomes possible (Figure 2). This 'splitting' becomes negligible for macrosamples, so that one can speak about size-induced bifurcation of the equilibrium lines at phase diagrams of nanosystems. This problem was explicitly formulated in [17] and later discussed in more detail in [20,21].

One of the substantial drawbacks of the mentioned approach was a lack of analytical formulae describing the combined size and depletion effects on a phase transformation. In particular, it was not clear what kind of size dependence correctly describes the depletion effects. In this paper, we present:

(1) a simple analytical approximation which is valid in a rather wide parameter range and gives an analytical description of decomposition in nanoparticles;
(2) a simplified analytical approximation for segregation in a nanoparticle without decomposition;
(3) an analytical description of simultaneous decomposition and segregation in a binary nanoparticle.

2. Decomposition without segregation

To illustrate the main ideas, we consider the decomposition of metastable (supersaturated) solid solution α' containing a finite total number N of A and B atoms, with initial

average concentration (atomic fraction) $\overline{C}$ of component B, into strictly stoichiometric phase 'i', with strictly fixed concentration C_i, and into depleted parent solution α. The phase diagram of this system for the concentration interval $0 < C < C_i = 0.5$ is shown in Figure 2. Below, we will see what is changed, and how, in the phase diagram for the case of finite particle size.

2.1. *Model and basic equations*

We consider homogeneous nucleation of the new phase inside a particle of radius R, which is thermodynamically favourable under the condition $\gamma_{i/\alpha} < \gamma_{i/V} - \gamma_{\alpha/V}$ for the surface tensions of interfaces i/α, i/V and α/V. We take into account depletion of the parent solution due to formation of the spherical nucleus (embryo) of phase 'i', containing n atoms, inducing depletion of the parent solution α. So far, we neglect a possible dependence of surface tension on composition which would lead to segregation and corresponding shift of composition in the 'bulk' of nanoparticle. The condition of a matter conservation, under the constraint of the stoichiometry of the i-phase, gives the concentration in the depleted parent phase as

$$C_\alpha = \frac{\overline{C}N - C_i n}{N - n}. \tag{1}$$

The change in Gibbs free energy induced by the nucleation is

$$\Delta G = g_i n + g_\alpha(C_\alpha) \cdot (N - n) - g_\alpha(\overline{C})N + \gamma \cdot 4\pi r_0^2 n^{2/3}. \tag{2}$$

Here, g_i and g_α are the values of Gibbs free energy per atom for the new and parent phases, γ is the surface tension of the interface i/α, $r_0 = \left(\frac{3\Omega}{4\pi}\right)^{1/3}$ is the atomic size and Ω is the atomic volume.

Further, we will use the ratio $\varepsilon \equiv n/N$ as a small parameter and will expand everything into series including second-order terms. Neglecting the higher order terms should be self-consistent, and we will formulate the self-consistency condition after obtaining analytical results. In particular, our approximation will be very questionable in the vicinity of the decomposition cupola top.

Simple algebra gives:

$$C_\alpha = \frac{\overline{C} - C_i\varepsilon}{1 - \varepsilon} \cong \overline{C} - (C_i - \overline{C})\varepsilon - (C_i - \overline{C})\varepsilon^2, \tag{3}$$

$$\Delta G \cong \gamma_i\alpha \cdot (4\pi r_0^2)n^{2/3} - \Delta g \cdot n + \frac{1}{2}(C_i - \overline{C})^2 g_\alpha'' \frac{n^2}{N}, \tag{4}$$

$$\Delta G/N \cong \gamma_{i\alpha} \cdot (4\pi r_0^2/N^{1/3})\varepsilon^{2/3} - \Delta g \cdot \varepsilon + \frac{1}{2}(C_i - \overline{C})^2 g_\alpha'' \varepsilon^2$$

$$= \frac{3\gamma_{i\alpha}\Omega}{R}\varepsilon^{2/3} - \Delta g \cdot \varepsilon + \frac{1}{2}(C_i - \overline{C})^2 g_\alpha'' \varepsilon^2. \tag{4'}$$

Here, $g''_\alpha = \frac{\partial^2 g}{\partial C^2}|_{\overline{C}}$ is the positive value for stable and metastable parent phases,

$$\Delta g = g_\alpha(\overline{C}) + (C_i - \overline{C})\frac{\partial g_\alpha}{\partial C}|_{\overline{C}} - g_i. \qquad (5)$$

is the bulk driving force for nucleation per atom of the nucleus (Figure 3).

Expansion like Equation (4′) was recently used in [22] for the description of void nucleation in a spherical particle supersaturated by vacancies from the surrounding growing phase.

The last term in Equation (4) is size-dependent (inversely proportional to total number of atoms, or, in other words, to the volume). In the limiting case, $N \rightarrow \infty$, one obtains the classical equation for nucleation barrier with positive surface term $\gamma \cdot 4\pi r_0^2 n^{2/3}$ hindering nucleation and negative (in decomposition region) bulk term $-\Delta g \cdot n$, leading to the nucleation inside the bulk decomposition cupola (binodal), determined by

$$\Delta g(C^{\text{bin}}, T) = 0, \text{ or } g_\alpha(C^{\text{bin}}) + (C_i - C^{\text{bin}})\frac{\partial g_\alpha(C, T)}{\partial C}|_{C^{\text{binod}}} - g_i(T) = 0. \qquad (6)$$

We will consider below a metastable parent phase, excluding spinodal decomposition, so that the second derivative with respect to concentration will be always positive and will also hinder nucleation. This situation is qualitatively similar to suppression of nucleation by a steep concentration gradient [23–27].

Let us denote $K \equiv (C_i - \overline{C})^2 g''_\alpha$. Note that $K > 0$. We will fix the average concentration and the temperature $\overline{C}, T$ of the particle and will change the total number N of
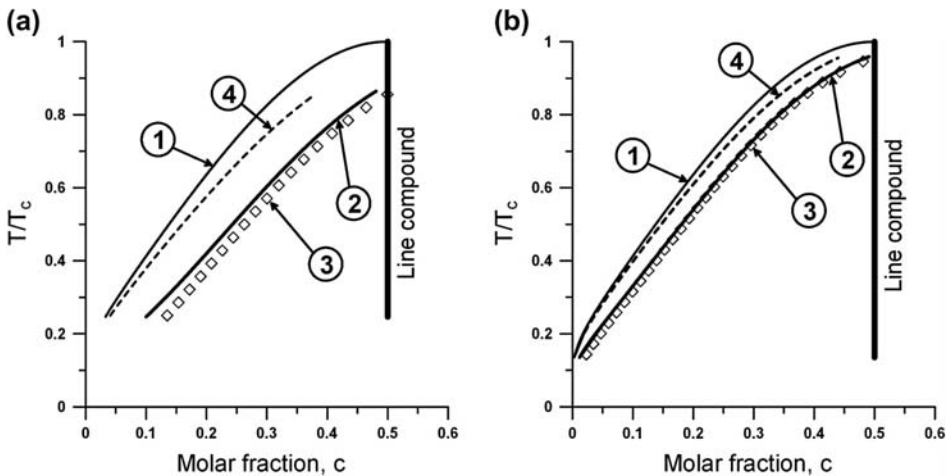

Figure 3. Phase diagram for different particle sizes: 1 – binodal for macrosystem (size R formally tending to infinity) calculated from common tangent rule, 2 – decomposition (solubility) curve (analytical), 3 – numerical calculation, 4 – depleted solution. (a) $\rho = 15$, (b) $\rho = 50$, where $\rho = \frac{RKT_c}{2\gamma\Omega}$.

atoms in this particle. Then, with increasing N, one by one, we derive the behaviours described by the curves 1–5 in Figure 1.

In case (1) of small N, the transformation is totally, thermodynamically forbidden, i.e. the value $\Delta G(n/N, \overline{C}, T)$ monotonically increases with growing embryo size (number of atoms) n. In case (2) of $N = N^*(\overline{C}, T)$, one has a first crossover of regimes, namely from totally suppressed transformation to possibility of metastable new phase formation. For this marginal regime, the curve $\Delta G(n)$ has an inflection point, at which both first and second derivatives are equal to zero:

$$\frac{\partial \Delta G(n)}{\partial n} = 0, \quad \frac{\partial^2 \Delta G(n)}{\partial n^2} = 0. \tag{7}$$

Substitution of Equation (4) into Equation (7) immediately gives:

$$n^* = \left(\frac{\frac{8}{9} \cdot \gamma 4\pi r_0^2}{\Delta g} \right)^3, \quad N^* = \frac{4K}{\Delta g} n^* = 4K \frac{\left(\frac{8}{9} \cdot \gamma 4\pi r_0^2 \right)^3}{(\Delta g)^4}. \tag{8}$$

For self-consistency, the condition

$$\frac{n^*}{N^*} = \frac{\Delta g}{4K} < 1 \tag{9}$$

should be satisfied (see below).

Another characteristic point (case 4 in Figure 2), $N = N^{**}(\overline{C}, T)$, determines a transition from the metastable new phase to the stable one, when the second minimum of $\Delta G(n)$ becomes the same depth as the first one. Starting from this point, decomposition becomes favourable. It means the following set of equations:

$$\Delta G(n) = 0, \quad \frac{\partial \Delta G(n)}{\partial n} = 0. \tag{10}$$

Substitution of Equation (4) into Equation (10) gives:

$$n^{**} = \left(\frac{\frac{4}{3} \cdot \gamma 4\pi r_0^2}{\Delta g} \right)^3 = \frac{27}{8} n^*, \tag{11a}$$

$$N^{**} = \frac{2K}{\Delta g} n^{**} = 2K \frac{\left(\frac{4}{3} \cdot \gamma 4\pi r_0^2 \right)^3}{(\Delta g)^4} = \frac{27}{16} N^*. \tag{11b}$$

For self-consistency, the condition

$$\frac{n^{**}}{N^{**}} = \frac{\Delta g}{2K} < 1 \tag{12}$$

should be satisfied (see below).

2.2. *Size-induced solubility shift*

Since Equation (11b) corresponds to equality between single-phase (first minimum $\Delta G = 0$ at $n = 0$) and two-phase states ($\Delta G = 0$ at $n = n^{**}$, when $C = C^{**}$), it is natural to treat it as a condition of solubility limit; for this, we rewrite it in a following form:

$$(\Delta g(C^{**}, T))^4 = \frac{2K(\overline{C}, T)}{N}\left(\frac{4}{3}\cdot\gamma 4\pi r_0^2\right)^3 = \frac{2(C_i - C^{**})^2 g_\alpha''(C^{**}, T)}{N}\left(\frac{4}{3}\cdot\gamma 4\pi r_0^2\right)^3. \quad (13)$$

It is natural that for the macroscopic samples ($N \to \infty$), Equation (13) is reduced to the usual binodal curve (6). Comparing Equation (13) with Equation (6), and assuming size-induced shift of the binodal, $\delta C^{**} \equiv C^{**}(T) - C^{\text{bin}}(T)$ as a small value with negligible second order, one obtains:

$$(\delta C^{**})^4 \left(\frac{\partial \Delta g}{\partial C}\bigg|_{\text{bin}}\right)^4 \cong \frac{2(C_i - C^{\text{bin}})^2 g_\alpha''(C^{\text{bin}})}{N}\left(\frac{4}{3}\gamma \cdot 4\pi r_0^2\right)^3.$$

(Namely, at the binodal curve, according to Equation (6), $\Delta g = 0$. Thus, the first non-vanishing term in the Taylor expansion is a product of the first derivative and the concentration shift.)

Taking into account that $\frac{\partial \Delta g}{\partial C} = (C_i - C)g_\alpha''$, we obtain the shift of the binodal:

$$\delta C^{**} \cong \frac{2}{N^{1/4}\sqrt{C_i - C^{\text{bin}}}}\left(\frac{\frac{2}{3}\cdot\gamma 4\pi r_0^2}{g_\alpha''(C^{\text{bin}})}\right)^{3/4} = \frac{2}{\sqrt{C_i - C^{\text{bin}}}}\left(\frac{2\gamma\Omega}{g_\alpha'' R}\right)^{3/4}. \quad (14)$$

Note that the size dependence, $\delta\tilde{N} \propto R^{-3/4}$, differs from well-known effect R^{-1}, arising from surface influence.

2.3. *"Splitting" of the shifted binodal*

In the bulk case, crossing the binodal means tending to supersaturation and, hence, the practically unchanged composition of the parent phase after precipitation of the practically zero volume fraction of the new phase. This situation changes dramatically in a nanosystem. Since the number of atoms in the formed new phase can be comparable with the total number of atoms, one cannot neglect depletion even just after reaching the solubility limit [17,21,20]. It means that one should distinguish the solubility limit and composition of the parent phase after decomposition. Thus, the shifted binodal is split: after reaching the solubility limit $C^{**}(T) = C^{\text{bin}}(T) + \delta C^{**}$, and formation of a stable particle of the new phase (second minimum at curve 4 at Figure 1), the parent phase will have a concentration (according to Equation (1))

$$C^{***}(T) = C^{\text{bin}}(T) + \delta C^{**} - \frac{C_i n^{**}}{N^{**}}. \quad (15)$$

Substitution of Equations (11) and (15) gives:

$$C^{***}(T) \cong C^{\text{bin}}(T) + \delta C^{**}\left(1 - \frac{C_i}{2(C_i - C^{bin})}\right). \tag{16}$$

2.4. *Self-consistency condition*

Conditions (9) and (12) of self-consistency (note that if condition (12) is fulfilled, then condition (9) is also fulfilled), taking into account a Taylor expansion of the driving force ($\Delta g \cong 0 + \delta C \cdot \frac{\partial \Delta g}{\partial C} = \delta C \cdot (C_i - C^{\text{bin}})g_\alpha''$), give:

$$\frac{\Delta g}{2K} \cong \frac{\delta C}{2(C_i - C^{\text{bin}})} < 1. \tag{17}$$

Combining Equation (17) with Equation (14), one obtains:

$$(C_i - C^{\text{bin}})^2 N^{1/3} > \frac{\frac{2}{3}\gamma \cdot 4\pi r_0^2}{g_\alpha''(C^{bin})}, \tag{18a}$$

or, in other form,

$$\frac{2\gamma\Omega}{R} < (C_i - C^{\text{bin}})^2 g_\alpha''(C^{\text{bin}}). \tag{18b}$$

All the curves depicted in Figure 3 satisfy condition (18), as was checked by numerical calculations in Section 2.5.

2.5. *Comparison with exact numerical result for regular solid solution*

We compared the just mentioned analytical results with the exact numerical result for the simple case when α-phase is a regular solid solution, and the Gibbs potential of the intermediate line compound is constant. It can be easily found that the results are determined by the dimensionless parameters $\rho = \frac{R \cdot kT_c}{2\gamma\Omega}$, and the "depth" of the intermetallic $\frac{g_i - g_\alpha(0)}{kT_c}$, where T_c is the maximum temperature of the decomposition cupola for the bulk case. In accepted notations, the expression for the Gibbs free energy change per atom, according to Equation (2), is $\frac{\Delta G}{NkT} = \tilde{g}_0 \cdot \varepsilon + \tilde{g}(c) \cdot (1 - \varepsilon) + \frac{3}{2}\frac{\varepsilon^{2/3}}{\rho} - \tilde{g}(c_0)$, where $\tilde{g}_0 = \frac{g_i - g_\alpha(0)}{kT} = \frac{g_i - g_\alpha(0)}{kT_c}\frac{1}{\tau}, \tilde{g} = \frac{4}{\tau}\left(\ln 2 + \frac{g_i - g_\alpha(0)}{kT_c}\right) \cdot c(1 - c) + c \ln c + (1 - c)\ln(1 - c)$ and $\tau = \frac{T}{T_c}$. In our calculations, we have chosen $\frac{g_i - g_\alpha(0)}{kT_c} = -1$. One can see that the analytic approximation works surprisingly well. The larger particle size is, the better the coincidence with the exact solution. It follows the exact solution well starting from $\rho \sim 20$, which corresponds (by the order of magnitude) to a real particle size about 10–100 nm. Indeed, if one supposes that the critical temperature is about 10^3 K, surface tension $\gamma \sim 1$ J/m^2, atomic volume $\Omega \sim 10^{-29}$ m^3, then at $R = 15$ nm, we have $\rho = 10.35$. It was found that the analytical approximation works surprisingly well even if the expansion parameter $\frac{n}{N}$ is not small: in the case when the size of precipitate almost reaches the size

of the particle, its value is close to unity, at that $C^{**} \sim C_i$. But, as follows from Figure 3 (curves 2 and 3), the relevance of the analytical approximation is still satisfactory.

3. Segregation without decomposition

Now, let the external surface tension linearly depends on the composition: $\gamma_{\alpha V}(C_\Sigma) = \gamma_B C_\Sigma + (1 - C_\Sigma)\gamma_A$, $\frac{\partial \gamma_{\alpha V}}{\partial C_\Sigma} = \gamma_B - \gamma_A \equiv -\Delta\gamma_\alpha$. Of course, a linear approximation is rather crude – therefore, results below are only qualitative. We suggest that all segregation proceeds with surface concentration C'_Σ in a narrow surface layer of width δ containing approximately $4\pi R^2 \delta / \Omega$ atoms. The fraction of atoms in the surface layer is

$$\beta = \frac{4\pi R^2 \delta}{4\pi R^3/3} = \frac{3\delta}{R}.$$

The Gibbs free energy of the system in this case is:

$$G = g_\alpha(C') \cdot (N - \beta N) + g_\alpha(C'_\Sigma)\beta N + \gamma_{\alpha V}(C'_\Sigma) \cdot 4\pi R^2. \tag{19}$$

Constraint of matter conservation gives:

$$C' \cdot (1 - \beta) + C'_\Sigma \beta = \overline{C} \Rightarrow \frac{\partial C'}{\partial C'_\Sigma} = \frac{-\beta}{1 - \beta}. \tag{20}$$

Minimization of function G in Equation (19) with account of constraint (20) gives the condition of equilibrium segregation in the nanoparticle:

$$\frac{\partial g_\alpha(C'_\Sigma)}{\partial C'_\Sigma} - \frac{\partial g_\alpha(C')}{\partial C'} = -\frac{\Omega}{\delta}\frac{\partial \gamma_{\alpha V}}{\partial C_\Sigma} = \frac{\Omega \Delta\gamma_\alpha}{g''_\alpha \delta}. \tag{21}$$

Assuming the second derivative g''_α is independent of concentration at least within the interval (C', C'_Σ), one gets the equilibrium concentrations:

$$C' = C - \frac{3\Omega\Delta\gamma_\alpha}{g''_\alpha R}, \tag{22}$$

$$C'_\Sigma = C + \frac{\Omega\Delta\gamma_\alpha}{g''_\alpha \delta}(1 - \beta), \tag{23}$$

$$C'_\Sigma - C' = \frac{\Omega\Delta\gamma_\alpha}{g''_\alpha \delta}. \tag{24}$$

4. Synergy of decomposition and segregation

Now let us have both, namely the decomposition inside a nanoparticle and segregation at the external surface of this particle (heterogeneous formation of the new phase at the surface will be discussed elsewhere).

The Gibbs free energy in this case is:

$$G = g_i n + g_\alpha(C') \cdot (N - \varepsilon N - \beta N) + g_\alpha(C'_\Sigma)\beta N + \gamma_{\alpha V}(C'_\Sigma) \cdot 4\pi R^2 + \gamma \cdot 4\pi r_0^2 n^{2/3} \quad (25)$$

with constraint of matter conservation:

$$C_i \varepsilon + C' \cdot (1 - \varepsilon - \beta) + C'_\Sigma \beta = \overline{C}. \quad (26)$$

First of all, we optimize the segregation at a fixed volume fraction ε of new phase. This gives

$$C'' = \frac{\overline{C} - C_i \varepsilon - \frac{3\Omega\Delta\gamma_\alpha}{g''_\alpha R}}{1 - \varepsilon}, \quad (27)$$

$$C''_\Sigma = \frac{\overline{C} - C_\varepsilon + (1 - \varepsilon - \beta)\frac{\Omega\Delta\gamma_\alpha}{g''_\alpha \delta}}{1 - \varepsilon}, \quad (28)$$

$$C''_\Sigma - C'' = \frac{\Omega\Delta\gamma_\alpha}{g''_\alpha \delta}. \quad (29)$$

Further, simple algebra using a Taylor series expansion in ε gives the following difference between Gibbs free energies with and without the new phase:

$$(G(\varepsilon) - G(\varepsilon = 0))/N = \frac{3\gamma_{i\alpha}\Omega}{R}\varepsilon^{2/3} - \Delta\tilde{g} \cdot \varepsilon + \frac{\widetilde{K}}{2}\varepsilon^2, \quad (30)$$

$$\Delta\tilde{g} = g_\alpha(\overline{C}) + (C_i - \overline{C})\frac{\partial g_\alpha}{\partial C}\bigg|_{\overline{C}} - g_i - \frac{3\Omega\Delta\gamma_\alpha}{R}(C_i - \overline{C}) = \Delta g - \frac{3\Omega\Delta\gamma_\alpha}{R}(C_i - \overline{C}), \quad (31)$$

$$\widetilde{K} = \left(C_i - \overline{C} - \frac{3\Omega\Delta\gamma_\alpha}{Rg''_\alpha}\right)^2 g''_\alpha = K \cdot \left(1 - \frac{3\Omega\Delta\gamma_\alpha}{Rg''_\alpha(C_i - \overline{C})}\right)^2. \quad (32)$$

Then, considerations, analogous to those in Section 2.2, give us the following expression for the shift of binodal containing two terms:

$$\delta C^{**} \cong \frac{2}{\sqrt{C_- C^{\text{bin}}}}\left(\frac{2\gamma\Omega}{g''_\alpha R}\right)^{3/4} + \frac{3\Omega\Delta\gamma_\alpha}{Rg''_\alpha}. \quad (33)$$

The first term is due to depletion of solute in the parent phase by the new phase. The second term is due to segregation and can be positive as well as negative.

The first term is larger than the second one or comparable with it at $R > \left(\frac{2\gamma\Omega}{g_\alpha''}\right) \cdot \frac{\Delta\gamma_\alpha}{\gamma_{i\alpha}}$, which is about couple of nanometers for typical parameter values.

5. Conclusions

The analytical description of the interrelations between the size effect, segregation and the decomposition in a small volume (e.g. a nanoparticle) is suggested. Size-induced shift of the solubility limit and splitting of binodal line would both be inversely proportional to the linear size to the power $\frac{3}{4}$ (or total volume to the power $\frac{1}{4}$) in the absence of segregation. Segregation adds a term inversely proportional to size. The analytical approach is applicable for comparatively large sizes or/and comparatively wide decomposition cupola (miscibility gap). In general, the presented approach analytically describes significant shifts of phase equilibrium for nanoparticles within the size range 10–100 nm. This approach should be generalized for the case of segregation at grain boundaries instead of the free surface [28] and heterogeneous nucleation in nanocrystalline materials. It seems also natural to extend our approach to the size effect on the spinodal curve which has been recently analysed in [29,30]. This will be done elsewhere.

References

[1] K.C. Lu, K.N. Tu, W.W. Wu, L.J. Chen, B.Y. Yoo and N.V. Myung, Appl. Phys. Lett. 90 (2007) p.253111.
[2] Y.C. Lin, K.C. Lu, W.W. Wu, J. Bai, L.J. Chen, K.N. Tu and Y. Huang, Nano Lett. 8 (2008) p.913.
[3] A.O. Kovalchuk, A.M. Gusak and K.N. Tu, Nano Lett. 10 (2010) p.4799.
[4] F. Baras and O. Politano, Phys. Rev. B 84 (2011) p.024113.
[5] S.C. Barron, R. Knepper, N. Walker and T.P. Weihs, J. Appl. Phys. 109 (2011) p.013519.
[6] B.B. Straumal, A.A. Mazilkin, S.G. Protasova, A.A. Myatiev, P.B. Straumal and B. Baretzky, Acta Mater. 56 (2008) p.6246.
[7] B.B. Straumal, B. Baretzky, A.A. Mazilkin, S.G. Protasova, A.A. Myatiev and P.B. Straumal, J. Eur. Ceram. Soc. 29 (2009) p.1963.
[8] B.B. Straumal, A.A. Mazilkin, S.G. Protasova, A.A. Myatiev, P.B. Straumal and E. Goering, Phys. Stat. Sol. B 248 (2011). p.581. doi: 10.1002/pssb.201001182.
[9] B. B. Straumal, S. G. Protasova, A. A. Mazilkin, E. Rabkin, D. Goll, G. Schütz, B. Baretzky, R. Valiev, J. Mater. Sci. 46 (2011). doi: 10.1007/s10853-011-5805-0
[10] C. Lemier and J. Weissmüller, Acta Mater. 55 (2007) p.1241.
[11] J. Weissmüller and C. Lemier, Philos. Mag. Lett. 80 (2000) p.411.
[12] J. Weissmüller and C. Lemier, Phys. Rev. Lett. 82 (1999) p.213.
[13] Y. Petrov, *Clusters and Small Particles*, Nauka, Moscow, 1986.

[14] A.I. Rusanov, Phase Equilibriums and Surface Phenomena, Leningrad, 1967.

[15] H. Ulbricht, J. Schmelzer, R. Mahnke, and F. Schweitzer, Thermodynamics of Finite Systems and Kinetics of First-order Phase Transitions, BSB Teubner, Leipzig, 1986.

[16] A.M. Gusak and A.S. Shirinyan, Met. Phys. Adv. Technol. 20 (1998) p.40, in Russian.

[17] A.S. Shirinyan and A.M. Gusak, Phil. Mag. A 84 (2004) p.579.

[18] B.B. Straumal, A.A. Mazilkin, S.G. Protasova, S.V. Dobatkin, A.O. Rodin, B. Baretzky, D. Goll and G. Schütz, Mater. Sci. Eng., A 503 (2009) p.185.

[19] B.B. Straumal, S.V. Dobatkin, A.O. Rodin, S.G. Protasova, A.A. Mazilkin, D. Goll and B. Baretzky, Adv. Eng. Mater. 13 (2011) p.463.

[20] A.M. Gusak, T.V. Zaporozhets, Y. Lyashenko, S.V. Kornienko, M.O. Pasichnyy and A.S. Shirinyan, *Diffusion-controlled Solid State Reactions,* in *Alloys, Thin-Films, and Nanosystems*, Wiley-VCH, Berlin. Chapter 13, 2010.

[21] A.S. Shirinyan, A.M. Gusak and M. Wautelet, Acta Mat. 53 (2005) p.5025.

[22] A.M. Gusak, F. Hodaj and T.V. Zaporozhets, Philos. Mag. Lett. 91 (2011) p.741.

[23] A.M. Gusak, Ukrainian Phys. J. 35 (1990) p.725, in Russian.

[24] P.J. Desré and A.R. Yavari, Phys. Rev. Lett. 64 (1990) p.1533.

[25] F. Hodaj, A.M. Gusak and P.J. Desré, Philos. Mag. A 77 (1998) p.1471.

[26] A.M. Gusak, F. Hodaj and A.O. Bogatyrev, J. Phys.: Condens. Matter 13 (2001) p.2767.

[27] F. Hodaj and A.M. Gusak, Acta Mater. 52 (2004) p.4305.

[28] R. Kirchheim, Acta Mater. 50 (2002) p.413.

[29] A.S. Abyzov and J.W.P. Schmelzer, J. Chem. Phys. 127 (2007) p.114504.

[30] A.S. Abyzov and J.W.P. Schmelzer, J. Chem. Phys. 134 (2011) p.054511.

Appendix
Derivation of phase equilibrium shift at synergic influence of depletion by precipitation and of segregation at external surface

Here, we analyse in more detail the expressions (30–32) for simultaneous action of depletion and segregation. As in all previous considerations, we will treat the phase separation as becoming possible if simultaneously the two conditions are satisfied: $\Delta G(n) = 0$, $\frac{\partial \Delta G(n)}{\partial n} = 0$ (see Equation (10)). The same transformations, as in Section 2.1, give:

$$N^{**} = 2\widetilde{K} \frac{\left(\frac{4}{3} \cdot \gamma 4\pi r_0^2\right)^3}{(\Delta \tilde{g})^4}.$$ (A.1)

To find the shift of phase line, we can rewrite this expression as

$$\Delta \tilde{g}\left(C^{**} + \delta C^{**}, \frac{1}{R}\right) = \left(2\widetilde{K} \frac{\left(\frac{4}{3} \cdot \gamma 4\pi r_0^2\right)^3}{N}\right)^{1/4}.$$ (A.2)

For the bulk case ($R \rightarrow \infty$), the phase equilibrium means zero driving force:

$$\Delta\tilde{g}\left(C^{**}, \frac{1}{R} \to 0\right) = 0. \tag{A.3}$$

Expanding the left-hand side of Equation (A2) into a two-dimensional Taylor series over small variables δC^{**} and $\frac{1}{R}$, taking Equation (31) and Equation (A3) into account and neglecting the higher orders of small variables ε, $\frac{1}{R}$ (squares and products), one obtains:

$$(C_i - C^{\text{bin}})g_\alpha''\delta^{**} - \frac{3\Omega\delta\gamma_\alpha}{g_\alpha''}\frac{1}{R} \cong \left(2K\frac{\left(\frac{4}{3}\cdot\gamma 4\pi r_0^2\right)^3}{R^3/r_0^3}\right)^{1/4}, \tag{A.4}$$

which immediately gives

$$\delta C^{**} \cong \frac{2}{\sqrt{C_i - C^{\text{bin}}}}\left(\frac{2\gamma\Omega}{g_\alpha''R}\right)^{3/4} + \frac{3\Omega\delta\gamma_\alpha}{Rg_\alpha''} \tag{A.5}$$